Solvent-induced local deformation zones in polyimide films adhered to a rigid substrate

A. C. M. YANG, H. R. BROWN
IBM Almaden Research Center, 650 Harry Road, San Jose, California 95120-6099, USA

Thin films of a polyimide (Ciba-Geigy XU293) adhered to rigid substrates developed special type of local deformation zones when immersed in xylene. These deformation zones were initiated because of the presence of the combination of xylene and the equi-biaxial tension resulting from the drying process. Their microstructure was strongly influenced by the local bonding to the substrate. In the bonded regions, the zones resembled a narrow trench containing deformed but unvoided material. In the unbonded regions, complicated fibrillar structure was observed in the much wider zones. Although they retained a smooth surface on the face in contact with the substrate in the bonded regions, the deformation zones released a significant amount of stress. The stress release was measured by a photo-elastic method and was found to be in excellent agreement with that calculated from the local thickness change assuming simple elasticity. Although not cracked, there were lines of weakness; after long soaking times the films cracked and delaminated along the defects.

1. Introduciton

Environmentally enhanced crazing or cracking in glassy polymers, especially organic solvent-induced failure, has been the focus of extensive research and is of continuing interest [1–6]. Generally, when a low molecular weight organic solvent diffuses into a polymer matrix, it plasticizes and swells the polymer. The critical strain or stress level required to form crazes or cracks is strongly depressed by the solvent, and, as a general rule, the failure mode switches towards a more brittle type of fracture. This solvent sensitivity usually restricts the uses of polymers in various engineering applications. In the recent development of microelectronic packaging, polyimides have emerged as a class of materials with a wide range of utility primarily due to their excellent high-temperature mechanical properties. Yet, problems of severe environmental stress cracking have been reported in some circumstances, particularly when a large equi-biaxial tensile stress is present in a thin polyimide film which adheres to a more rigid substrate. Previous research work on environmental stress cracking has concentrated on the free standing films or bulk specimens. However, for adhered films the mechanics of fracture and deformation are very different because of the effect of the adhesion at the polymer/substrate interface [7]. The modification of the solvent diffusion into the now partially shielded polymer film will also change the mechanics. It is the purpose of our current study to investigate the phenomenon and explore the fundamental implications of the solvent-induced deformation in this particular system.

2. Experimental procedure

Ciba-Geigy polyimide (XU293) in solvent γ-butyrolactone was kindly supplied by Drs P. Agostino and G. Czornyi of IBM, GTD at East Fishkill, New York. Thin polyimide films were prepared on glass slips by spin coating followed by drying at high temperatures on a hot plate: first at 85° C for 15 min, then 150° C for 30 min, and finally 230° C for 30 min. The speed of the spinner was fixed at 3×10^3 r.p.m., and the film thickness was controlled by the solvent concentration in the solution for the thickness regime from 0.15 to 10 μm. Thicker films (15 to 20 μm) were made by first drying one layer then recoating. Further coating of these thick films, however, was difficult because the pre-existing dried film cracked when in contact with the solution. The thickness of the films was measured using a Tencor Alpha-Step instrument.

Line defects, the main subject of this paper, were nucleated from the foreign inclusions and the sample edges when the thin adhered polyimide films were immersed in xylene. To control defect nucleation, small holes with a diameter ranging from 50 to 100 μm were usually introduced into the central region of the film with the tip of a razor blade. After the xylene immersion, the polyimide film dried quickly in air and was observed by a Jena polarized light microscope and by a Phillips 505 scanning electron microscope. With the Jena Interphako optical microscope, the birefringence was measured by an Ehringhaud quartz compensator and the refractive index by the interference method.

Before any xylene contact, the polyimide films could be peeled off the substrates so that the stress optical coefficient and the Young's modulus could be determined with a Polymer Lab Minimat strain frame. The stress optical coefficient was found to be 1.2×10^{-4} MPa^{-1} and the Young's modulus, E, to be 2000 MPa. Free-standing films were also produced so that their xylene-induced deformation could be compared with that of the adhered films. The dried film was carefully peeled off the substrate and placed on a

0022–2461/88 $03.00 + .12

piece of copper grid. The copper grid had been previously annealed at high temperature to give it ductility and the grid bars had been coated with a thin layer of epoxy as the adhesive so that the film would be held firmly to the grid when the epoxy was cured. Stress could then be introduced in the film by pulling the copper grid. This system was designed so that the stress was maintained in the substrate-free films during observation [8].

3. Experimental results

3.1. Optical microscopy

3.1.1. Bonded Films

After short immersion in xylene at room temperature, line defects that looked like thin cracks, grew radially from the foreign inclusions or the introduced initiator holes, reflecting the equi-biaxial nature of the stress in the film. These line defects, shown in Fig. 1, appeared bright between crossed polars, implying that they contained oriented material and hence were not true cracks but were some form of local deformation zones. In Fig. 1 the regions immediately neighbouring the defects also showed birefringence. They formed much wider, but more diffuse and less bright, linear bands which had a constant width except in the region near the tip. Photoelastic examination revealed that the tensile stress in the bands was lower in the normal direction than in the length direction. Thus these bands could be considered to be the regions where the initial stress was released by the formation of the line defects. They will be discussed in more detail later.

A pre-existing line defect could trap the other growing ones. Apparently following the route guided by maximum principle stress, as the tip of the new defect approached one deformation zone, it curved toward the latter and stopped after intersecting it at an angle of 90°, Fig. 2. The "trapping process' usually began when the two defects were within a distance of one to three times the width of the diffuse band. The stress state at the tip of the line defect apparently was complicated. In some circumstances, when a pair of defects approached each other, they repelled each other causing the change in their growth directions. Similarly, a tiny defect which was newly initiated

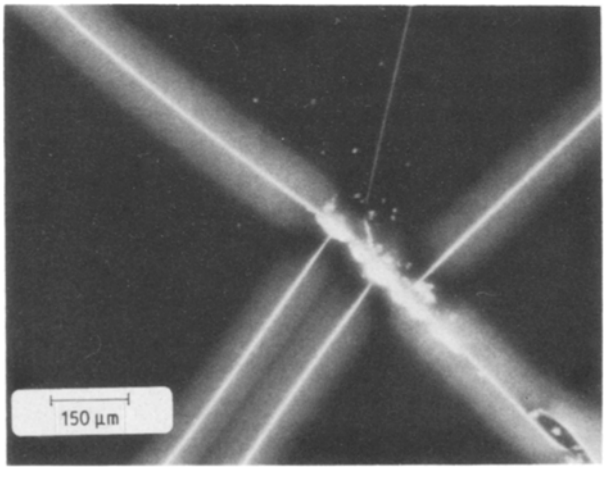

Figure 1 Polarized micrographs of the xylene-induced defects and the associated diffuse bands in coated polyimide films. The defects were initiated from heterogeneous interfaces.

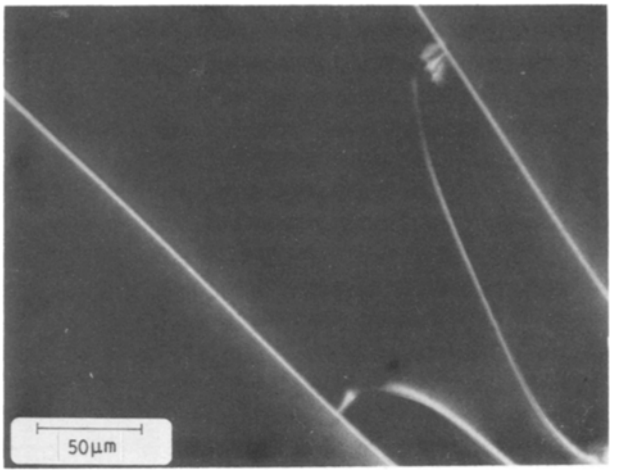

Figure 2 Two growing line defects stopped at the positions where two pre-existing ones are located.

within the diffuse band of another was apparently expelled away from the band when it subsequently grew.

The growth of the deformation zone modified the local stress distribution in its immediate neighbourhood. When an opening was formed, the initial state of the equi-biaxial tensile stress changed so that in the direction normal to the deformation zone the stress component decreased while in the length direction the stress was mostly preserved. This stress relief caused the birefringent diffuse band associated with the line defects, as mentioned earlier. The higher refractive index was parallel to the length direction in the diffuse band, indicating that, as the stress-optical coefficient is positive, the maximum stress was parallel to the deformation zone. The pattern of birefringence in the diffuse band was constant along the band except near the tip. However, the birefringence decreased with distance from the defect as the adhesion to the substrate ensured that the stress relief was only close to the defect. The birefringence was measured as a function of distance from the defect using a quartz compensator. The results are shown in Fig. 3. The stress decrease in both the normal and the length directions could then be derived from data in Fig. 3. The local

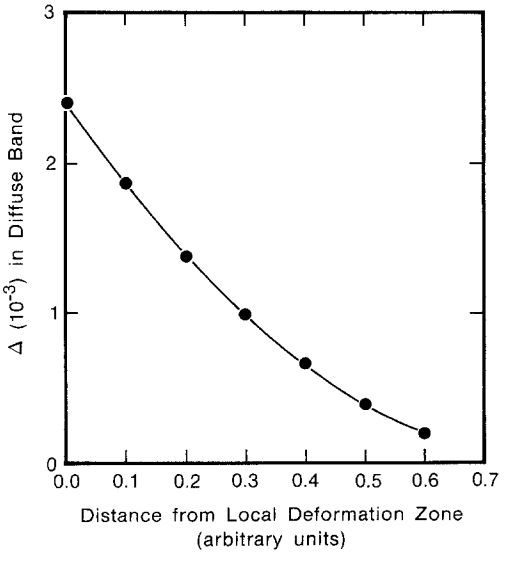

Figure 3 The birefringence in the diffuse band decreases as the distance from the defect increases.

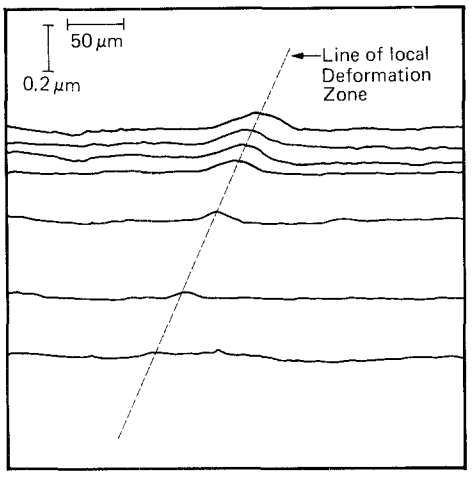

Figure 4 The α-step tracings across a xylene-induced defect. The defect runs about 60° to the scan direction.

film thickness was found to increase in the areas close to the deformation zones shown in Fig. 4. This local thickness change which was caused by Poisson's ratio effects provided another piece of information, independent of the birefringence, for the measurement of the stress decrease.

It may be assumed that the material response was elastic and that plane stress condition applied. The stresses σ_{11} and σ_{22} in the diffuse band can be expressed as

$$\sigma_{11} = \{\sigma_0(1 - \nu) - \sigma_d\}/(1 - \nu)$$
$$\sigma_{22} = \{\sigma_0(1 - \nu) - \nu\sigma_d\}/(1 - \nu) \quad (1)$$

where 1 denotes the normal direction and 2 the length direction of the band. Here σ_0 is the initial equi-biaxial tension in the film, ν the Poisson's ratio, and σ_d a positive quantity defined as $\sigma_{22} - \sigma_{11}$, obtainable directly from the birefringence and the stress optical coefficient. To derive Equation 1, we have used the fact that the strain in the length direction is zero. The

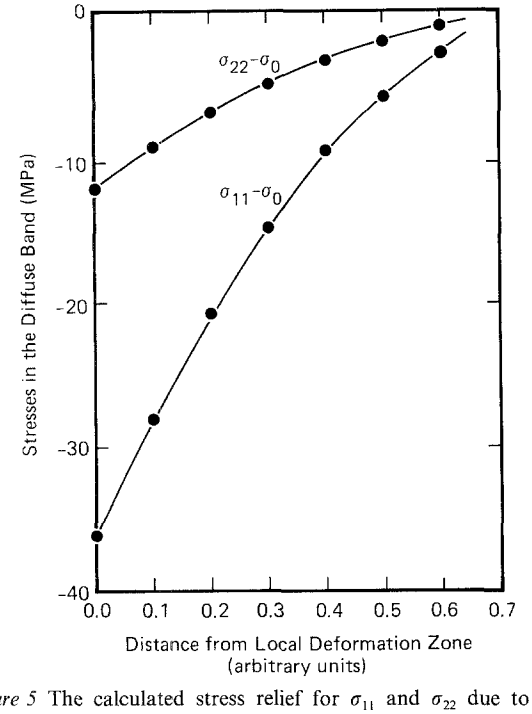

Figure 5 The calculated stress relief for σ_{11} and σ_{22} due to the formation of the xylene-induced defect as a function of the distance from the defect.

initial stress, σ_0, was measured by a bending beam method and was found to be approximately 65 MPa [9]. The Poisson's ratio was assumed to be 0.33. The stress σ_{11} as a function of the distance from the defect was obtained using Equation 1 and is plotted in Fig. 5. The stress decrease at the defect zone was around 30 MPa, about a 50% reduction of the initial value.

The local thickness change in the diffuse band was used to confirm this result. Using the same assumptions, the thickness change, δ, due to the local stress decrease can be written as

$$\delta = \{\nu(1 - \nu)\}\Delta\sigma_{11}\tau E \quad (2)$$

where E is the Young's modulus and τ the initial film thickness. The number δ is positive and was calculated to be around 60 nm from the measured value of $\Delta\sigma_{11}$ at the defect. This number was in excellent agreement with the thickness profile across a defect shown in Fig. 4, which also showed a maximum at the defect with a height of approximately 60 nm.

The nucleation and growth of the line defects was strongly dependent on the film thickness. It became increasingly difficult to grow the line defects by xylene immersion in the thinner films. No line defects were ever observed in films thinner than 2 μm. In the thick films, approximately between 8 and 20 μm thick, the defects nucleated within a minute after immersion in xylene and then grew rapidly, quickly encompassing the whole specimen of dimensions of 25 mm × 25 mm. The diffuse bands of the defects in these thick films were wide (~ 70 μm wide for 10 μm thick films) and bright, whereas in the thinner films, below 4 μm thick, it was very difficult to grow the defects. In this case even after more than 10 h immersion in xylene, the defects were very short, say ~ 20 μm, and the diffuse bands were insignificant, with a width of only about 4 μm. This strong thickness effect could be explained by a fracture mechanics analysis for a strain energy release rate-controlled "crack" growth and will be discussed in a separate paper [10].

The line defects obviously acted as the crack precursors. When the films of thickness 20 μm were immersed in xylene for 20 min, extensive debonding occurred starting from the edges of film and true cracks propagated along the defects causing serious delamination as shown in Fig. 6.

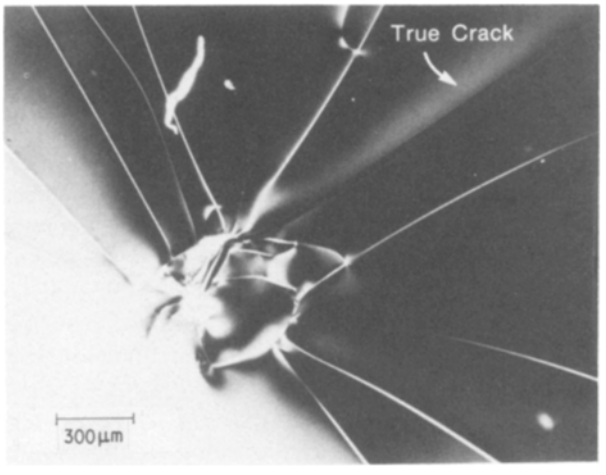

Figure 6 A true crack propagating from an initiator hole along a defect in a thick film (20 μm) after immersion in xylene for 20 min.

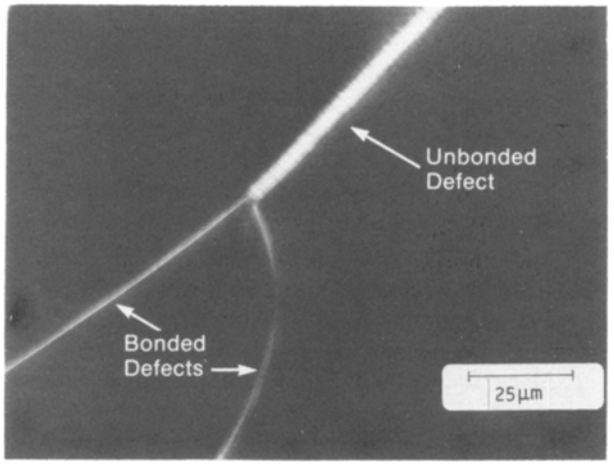

Figure 7 Optical micrographs showing a line defect travelling from the mechanically "debonded region" around a hole to the bonded region.

3.1.2. Unbonded films

The local bonding to the substrate did not affect the direction of propagation of the line defects: however, it dramatically changed their microstructure. For example, when immersed in xylene, the line defects could easily penetrate the small unbonded regions around the initiator holes, where the film had been mechanically disturbed prior to the xylene immersion, and propagate into the outer bonded regions without changing direction. But, as clearly shown in Fig. 7, the section in the unbonded region ("unbonded defect") was very different in appearance from that in the bonded region ("bonded defect"). In a striking contrast to the bonded defect, the unbonded defect was much wider and demonstrated a fibrillar structure. The diffuse band associated with the bonded defect disappeared here. This indicated a de-localized stress release in unbonded films.

A characteristic of anisotropic voided structure such as crazes [11] is that they show form birefringence whose presence can be detected by observing the effect of imbibing fluids into the structure. Using xylene ($n_D = 1.50$) as an imbiding liquid, the birefringence in the "unbonded defects" decreased dramatically as the liquid was applied covering the defects. When the liquid evaporated, however, the birefringence in the "unbonded defects" returned to its initial value. There was therefore a considerable form birefringence component indicating that these structures were voided. On the other hand, the "bonded defects" did not show any detectable form birefringence using this method. This indicated that unlike the unbonded defects, the bonded defects were not voided. The optical properties of the form birefringence in the unbonded defects were not typical of a simple birefringent structure in that they could be "compensated" in both the normal and length directions. This implies that they did not have a simple fibrillar structure. The orientional component of the birefringence in the unbonded defects, obtainable from the liquid-filled structure was 11×10^{-3} and indicated that the material was oriented normal to the defect. The opening in the bonded defects was so small, around 0.2 μm, that optical birefringence measurements were difficult.

Although they demonstrated a very different microstructure, the bonded defects could be the precursors of the unbonded defects. If the polyimide films were dried only at 85° C, the adhesion of the films to the substrates was much weaker than that of the films dried using the standard heating cycle. This meant that the unbonded regions could extend as the adhered films were immersed in xylene. Under these circumstances, the defects initially in the bonded regions were observed to be gradually converted into unbonded defects. The adhesion of the substrate apparently had restricted the deformation of the immersed films and thus prevented the films from voiding.

3.1.3. Free-standing films

For comparison purposes, free-standing films on copper grids were tested. Dry films of two different thicknesses, 10 and 0.75 μm, were strained uniaxially in tension up to a strain of approximately 8%. Around the inclusions and the initiator holes, shear deformation zones [12], another type of deformation mode, were produced which, when matured, broke to form diamond-shaped cracks [13] with a front angle of approximately 30° to 40°, see Fig. 8. Although these shear zones in both the free polyimide films were qualitatively similar, they were more "localized", and harder to nucleate and grow, in the thick films. The degree of orientation in the thin-film shear deformation zones was uniform, with a birefringence of approximately 32×10^{-3}. In the case of the thick film, the birefringence varied from $\sim 30 \times 10^{-3}$ in the regions near the diamond-shaped crack to $\sim 11 \times 10^{-3}$ in the region close to the undeformed areas.

When these uniaxially deformed free-standing films were immersed in xylene for 10 min, many crazes were formed which ran in the direction perpendicular to the initial tensile axis. These crazes were long, encompassed the whole film square, and many of them had broken to form large voids. The craze fibrils were huge and clearly visible even under an optical microscope, as shown in Fig. 9. Most of the wide crazes, however, had undergone extensive fibril coalescence [14] with a

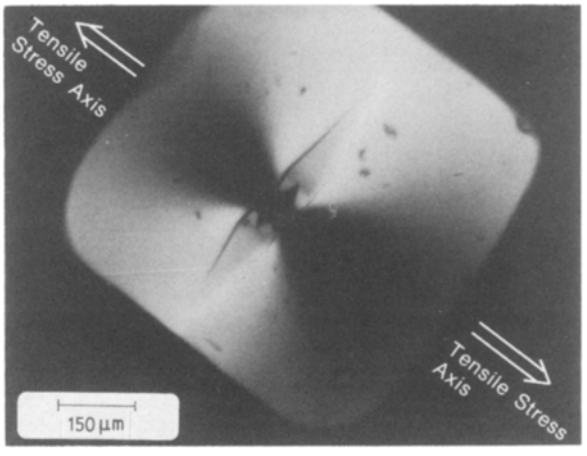

Figure 8 Shear deformation zones growing from the tips of an initiator hole in a free-standing film (10 μm). The film was subjected to a strain of 8% under the strain rate of 1.25% min^{-1}.

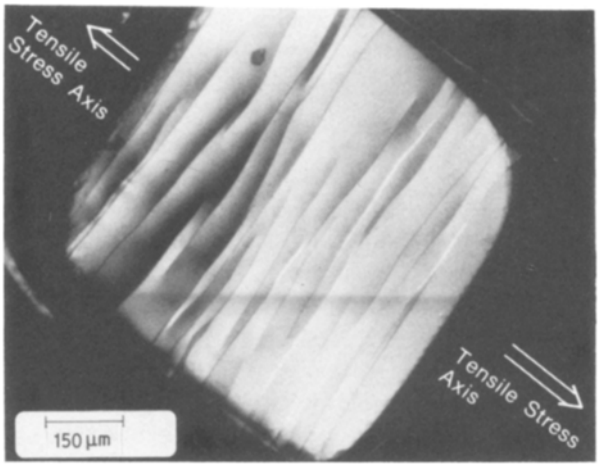

Figure 9 Optical micrographs of the crazes in a free-standing film (8 μm) generated after 10 min immersion in xylene. The film was deformed to a strain of 8% (strain rate = 1.25% min^{-1}) prior to the immersion.

"skin layer" covering most of the area of the crazes. The volume fraction of the crazed matter was obtained from the refractive index and found to be around 0.3, close to that found in many glassy polymers. The crazes had an orientation birefringence which ranged between ($\sim$ 10 to 16) $\times$ 10^{-3}, a value quite close to that in the debonded defects. The form birefringence in the free-standing crazes was measured between 0 to approximately 40 $\times$ 10^{-3} depending on the extent of coalescence. The higher refractive indices of both the orientation and form components were parallel to the fibril axis.

3.2. SEM

A scanning electron microscope was employed to examine further the microstructure of the bonded and unbonded defects in the adhered films. A bonded defect showed a narrow sharp trench on the surface, as shown in Fig. 10a, confirming the previous optical observation that the defects contained material. The surface topography in a bonded defect was difficult to access using SEM, because of the very narrow opening, around only 0.2 μm or less, and thus the overwhelming shadowing of its "banks". At the tip of the defect, Fig. 10b, we observed a gradual regression of the trench into the smooth surface, In this region, the surface in the trench was smooth, showing no surface features. Close to the initiator holes where the films were unbonded, this simple "trench" of the bonded

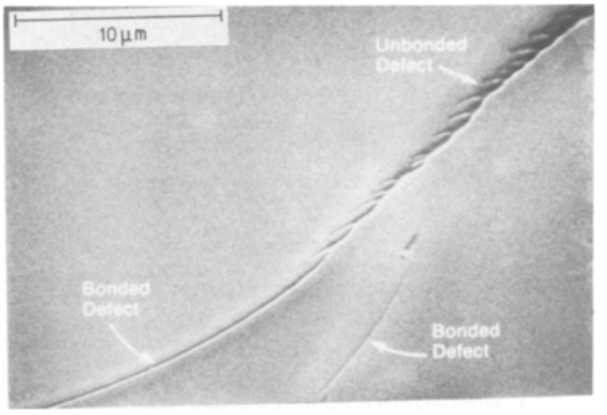

Figure 11 SEM topography of a line defect across the boundary between the bonded and the unbonded regions.

defects transformed into a structure unfamiliar in free-standing polymer films. Fig. 11 showed a line defect running across the bonded/unbonded boundary. In the section of the unbonded region, the surface topography consists of parallel "ridges" packed in a "trench" with the "ridges" perpendicular or sometimes tilted at an angle with respect to the trench, see Fig. 12. The trenches had a width of about 1 to 2 μm and the whole internal structure was below the film surface. The spacing between the ridges was approximately constant along the trench length. For each ridge, groups of small and narrow surface lumps branched out from the top line of the ridge and extended to the slope forming tree-like wrinkles. The wrinkles looked like partially fibrillated matter spread and fused on to a plane surface.

After observation of its surface the film was gently peeled off the glass substrate and the bottom surface of the film was examined by SEM. We noticed that while the xylene-induced defect in the area near the initiator hole (the debonded region) maintained an indented topography (the "ridge-and-valley" structure), as soon as it crossed the bonded/debonded boundary, the line defect had a flat bottom surface, virtually un-deformed except for only several small mild lumps and some tilted marks distributed along the zone near the boundary. This is shown in Fig. 13. The lumps and the dark marks became increasingly unresolvable as the scanned area moved away from the boundary into the bonded region. Near the boundary, those features spanned a width of approximately 2 μm, a space larger than its counterpart

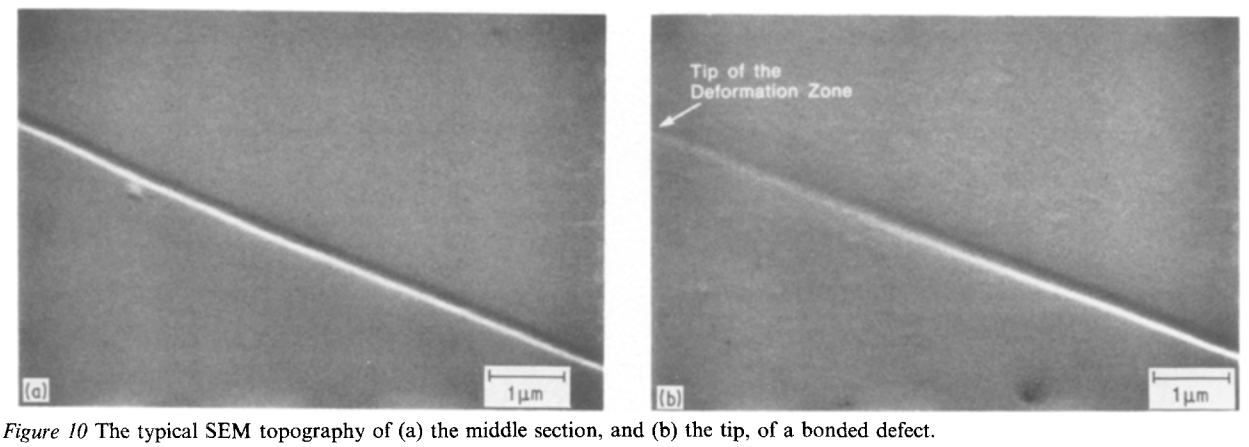

Figure 10 The typical SEM topography of (a) the middle section, and (b) the tip, of a bonded defect.

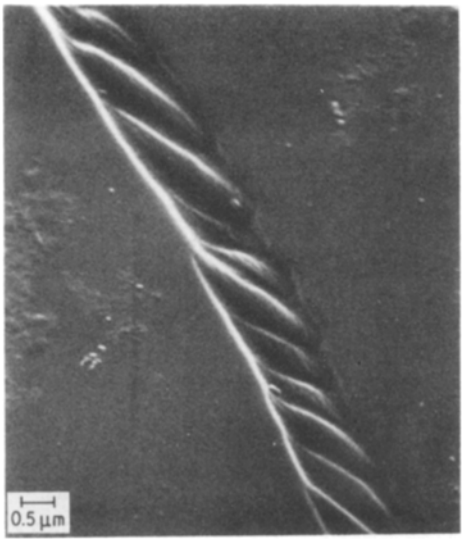

Figure 12 Scanning electron micrographs of the unbonded defects.

appeared on the free surface. The origin of these features is not yet completely clear; however, the marks might suggest some information of the internal structure of the xylene defects on the adhered region.

In an effort to explore the internal structure of the bonded defects, the films containing the xylene-induced defects were peeled from the substrate and mounted on copper grids. After application of a small uniaxial tensile strain, the samples were immersed in xylene. Many crazes quickly developed in the films and the pre-existing line defects opened up to form fibrillar zones. Some of these "crazed" line defects were broken down which permitted estimation of the depth of the trenches. The depth of this indentation in the bonded defects was found to be between 1 and 2 μm in a 10 μm thick film.

4. Discussion

From the results in the previous section, the microstructure of a bonded defect induced by xylene can be described as a very narrow trench with a yielded, but unvoided, material underneath the surface of the trench. The formation of this structure has been shown to release a significant amount of the stress. The fact that it is still load bearing is evident from the observation that the bonded defects can continuously deform to convert into a fibrillar structure when the bonding to the substrate fails. The unbonded defects can be viewed as "crazes" because they show fibrillar structure. Furthermore, the similarity of their orientation birefringence to that in crazes in the free-standing films suggests that unbonded defects and crazes are formed by similar molecular mechanisms. We have also noticed the gradual transition from the "craze-like" unbonded defect to the bonded defect, demonstrated in Fig. 11, where the morphology of the defects is similar to, but much coarser than, that of a "finger growth" craze [15]. This provides another clue that the bonded defects are possibly the "primordial" form of the unbonded defects. The adhesion to the substrate restricts the opening and hence full-scale propagation of the "fingers" and thus only allows the growth of one finger.

The driving force for the formation of these defects is clearly the tensile stress developed from the drying process of the films, together with the plasticization effects of the xylene. The requirement for the presence of the tensile stresses is demonstrated by the fact that both bonded and unbonded defects show an opening on the free-surface. It had been shown [16] that the xylene diffuses into the adhered polyimide coatings by following Case II diffusion. The molecular transport process is slow, requiring approximately 25 h at room temperature to saturate the 10 μm thick films. The weight gain was approximately 25%. A compressional stress generated by the swelling in the outerlayer from this slow sorption is thus unlikely to be responsible for the fast initiation of these defects. However, a stress-enhanced diffusion of the xylene, and hence the fast plasticization and deformation at the stress concentrations might be involved in the formation of the defects. The surface structure in the unbonded defects qualitatively resembles the methanol-induced "crazes" in the pre-existing shear bands in polystyrene (PS) or poly(methylmethacrylate) (PMMA) which were formed under a slight tension [17]. It is therefore thought possible that shear yielding also participates in the complicated deformation process.

The effects of the interfacial adhesion to the substrate are large here. The adhesion differentiates the bonded and the unbonded defects by reducing the extent of strain softening available, restricting the opening, and protecting the film from voiding because the bottom layer was constrained in space. The bonded

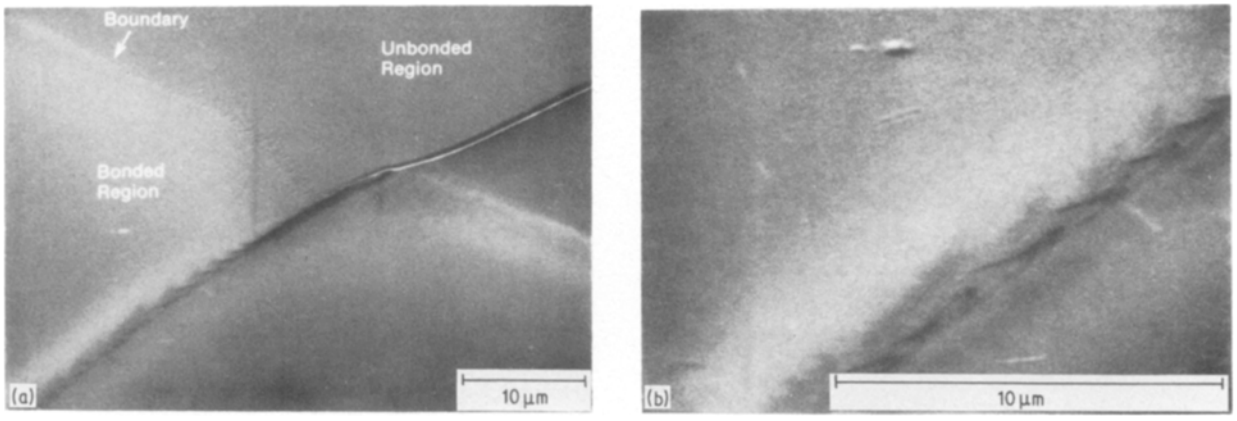

Figure 13 Scanning electron micrographs of the underside of the xylene-induced defects. Note the abrupt change in topography in (a), as the defect crosses the bonding/debonding boundary. The titled dark marks clearly visible in (b) suggest some deformation in the defect.

defects have exhibited an virtually intact surface in the underside. A fracture mechanics approach can explain this effect. Gecit [7] has shown that the stress intensity factors $K(b)$ in the thickness direction for an edge crack in a surface layer bonded into a more rigid half plane approaches to zero as the depth of the crack, b, moves to the total film thickness. This means that a coating on a more rigid substrate is partially protected from through-thickness cracking.

The wide diffuse bands associated with the defects are clearly created by the stress relief of the defects causing local optical anisotropy and thickness change. The fact that their birefringence does not change along the zone length implies that the stress at the defect is constant along its length. Thus the Dugdale model [18] of stress distribution at a crack tip in a yielding material, which is widely used in craze stress analysis, is probably useful here. By using this simple model, we should be able to connect the defect propagation speed with the fracture energy release rate for the study of the fracture mechanics of adhered layers.

5. Conclusions

1. Xylene immersion causes a polyimide film which adheres to a rigid substrate to form a unique type of local deformation zone. The mechanism of deformation of this zone is probably related to crazing. The large equi-biaxial tension in the film is responsible for the development of these defects.

2. The microstructure of the deformation zone was strongly influenced by the adhesion condition at the interface.

3. The formation of the xylene-induced defects releases a significant amount of stress. The stress relief can be measured by a photo-elastic method. The result is in excellent agreement with that calculated from a local thickness change by assuming simple elasticity.

4. Under uni-axial tension free-standing polyimide film is deformed by local shear yielding. But when in contact with xylene, it undergoes extensive crazing.

Acknowledgements

We gratefully acknowledge the financial support of IBM, GTD at East Fishkill, New York and the helpful discussion with Dr. G. Czornyj and his research group. The assistances of J. A. Logan and J. Duran in the operations of the optical microscope and SEM, respectively, are acknowledged.

References

1. G. A. BERNIER and R. P. KAMBOUR, *Macromol.* **1** (5) (1968) 393.
2. E. H. ANDREWS and L. BEVAN, *Polymer* **13** (1972) 337.
3. R. P. KAMBOUR, C. L. GRUNER and E. E. ROMAGOSA, *J. Polym. Sci. Polym. Phys. Edn* **11** (1973) 1879.
4. J. G. WILLIAMS and G. P. MARSHALL, *Proc. R. Soc. A* **342** (1975) 55.
5. Y. IMAI and N. BROWN, *J. Mater. Sci.* **11** (1976) 417.
6. E. J. KRAMER, in "Developments in Polymer Fracture", edited by E. H. Andrews, Ch. 3, (Applied Science, Barking, UK, 1979) p. 55.
7. M. R. GECIT, *Int. J. Eng. Sci.* **17** (1979) 287.
8. B. D. LAUTERWASSER and E. J. KRAMER, *Philos. Mag. A* **245** (1979) 312.
9. C. FERGER, personal communication (1985).
10. H. R. BROWN and A. C. M. YANG, in preparation.
11. H. R. BROWN, *J. Polym. Sci. Polym. Phys. Edn* **17** (1979) 1417.
12. C. S. HENKEE and E. J. KRAMER, *ibid.* **22** (1984) 721.
13. P. L. CORNES and R. N. HAWARD, *Polymer* **15** (1974) 149.
14. A. C. M. YANG and E. J. KRAMER, *J. Polym. Sci. Polym. Phys. Edn* **23** (1985) 1353.
15. A. M. DONALD and E. J. KRAMER, *Philos. Mag. A* **43** (1981) 857.
16. A. C. M. YANG and H. R. BROWN, unpublished.
17. J. C. M. LI, *Polym. Eng. Sci.* **24** (1984) 750.
18. D. S. DUGDALE, *J. Mech. Solids* **8** (1960) 100.

Received 1 December 1986
and accepted 29 January 1987